Examining the Chromophoric Geochemistry of Red Beryl from the Three Known Localities

Kyriaki T. Papageorgiou

Advisors: Dr. Philip M. Piccoli, Dr. Richard Ash

GEOL394: Senior Thesis

University of Maryland, College Park
Department of Geology

April 29th, 2025

Table of Contents

Scientific Abstract

Red beryl, formerly known as bixbite, is the rarest type of beryl and possibly the rarest gemstones known. Sought after for both its beauty and its rarity, it is estimated to be worth over one hundred times more than gold, and for every 150,000 diamonds found, one red beryl is found (Edge, 2002). On average, high-quality, faceted specimens sell for about $2000 a carat. Red beryl has been documented in three localities worldwide, two in Utah, and one in New Mexico. Despite its extreme value and rarity, the formation of red beryl is not well understood.

For the first time, complicated red beryl trace element and chromophore geochemistry of all three localities have been analyzed, observed, and compared to determine the if chemistry is distinguishable between the localities. The selected samples have been compared to elemental abundance data of other varieties of beryl from around the world. These data have been pulled from Gavrilchik et al. 2023. The method for this study was LA-ICP-MS analyses of over thirty elements across eight samples of red beryl. Comparing the major, minor, and trace elements of red beryl from all localities display significant range as well as overlap, and individual samples are both visually and chemically heterogenous from core to rim. The analyzed samples exhibit enrichment and depletion in the same chromophore elements, LREE's, HREE's, and other minor trace elements. Other varieties of beryl, such as emerald (green), aquamarine (blue), heliodor (yellow), goshenite (clear), and pezzottaite (pink) differ in many the chromophore constituents. In comparison to other beryl, emerald and aquamarine have a significantly higher concentration of chromium (being the common coloring agent of emerald and sometimes aquamarine), red beryl has a miniscule amount of chromium. Red beryl also shares some similarities with beryl varieties that have their own unique traits. Pink beryl, or pezzoattaite, is distinctive in its high cesium content, which is also believed to be the coloring agent (Gavrilchik et al. 2023).

Plaintext Abstract

Beryl is a mineral and a resource with a variety of uses and applications. Beryl, along with bertrandite, are two major sources of beryllium. Pure beryllium and beryllium alloys are used in aircraft instruments, satellites, spacecraft, rocket propellants, navigational systems, and other complex machinery.

Beryl is a common mineral. It comes in a wide array of colors, forms in hexagonal columns, and has a hardness of 7.5-8.0, all of which make it a coveted gemstone in the jewelry industry. Green beryl is known as emerald. Similarly, blue beryl is known as aquamarine. Green, blue, yellow (heliodor), clear or white/opaque (goshenite), pink (pezzottaite, morganite), and red beryl are often zoned—containing multiple colors and hues within a single crystal.

Despite the commonness of beryl, red beryl is certainly the rarest beryl, if not one of the rarest minerals in the world. Faceted, gem-quality specimens can be priced at as much as $2000 per carat. Red beryl is only known to occur in three localities worldwide—two in Utah and one in New Mexico. Despite its value and rarity, not much is known about the unique geochemical processes that contribute to the creation of red beryl.

Eight red beryl samples were collected from the three known localities for this study. The method used for this study, Laser Ablation-Inductively Coupled Plasma-Mass Spectrometry (LA-ICP-MS), offers the ability to measure minor and trace elemental concentrations within a sample. The goal of this study is to do what has not been done before-- to study the geochemistry of the chromophore elements (as well as elements that may sometimes act as chromophores in other minerals) in red beryl from each locality, as well as see how these abundances differ from the other beryl varieties. Among red beryl, data collected

suggest that the formation of the three beryl was similar chemically—being enriched and depleted in the same minerals and minerals groups, though, their chemistry is a bit more complicated than that. Though there is a large overlap in the measured elemental abundances of the analyzed samples, there is also a significant amount of displayed among the localities and the individual crystals themselves. Many of the red beryl grains analyzed exhibit both visible and chemical zoning, with some elements more enriched in the core, or the rim, and other elements that are constant throughout the grain despite the zoning. Through this study, more of the intricacies of red beryl geochemistry will be unveiled, and provide a better understanding of the unique process and environment in which red beryl formed.

Introduction

The occurrence of red beryl has been documented at only three locations worldwide. These locations include the Thomas Range in Utah, the Wah Wah Mountains in Utah, and the Paramount Canyon of the Black Range in New Mexico (**Figure 1**). Historically, gem-quality red beryl has been mined industrially in the Wah Wah Mountains, and is the only locality that has produced gem-quality crystals. The Wah Wah Mountains are still undergoing exploration and extraction for red beryl to this day.

F.1: Google satellite imagery of the western USA, displaying the three red beryl localities.

Red beryl is hosted in topaz rhyolite in the western United States. Formed in the middle Tertiary, the Thomas Range, Wah Wah Mountains, and the Black Range mark only three of many rhyolites and topaz rhyolites formed by slab-rollback volcanism--an event in which a subducted portion of the Farallon Plate began to melt and rise through the thick felsic crust of

the North American Plate, causing a series of felsic and intermediate volcanoes throughout western North America.

The nominal chemical formula of red beryl is $Be_3Al_2Si_6O_{18}$. It has also been known to co-occur with manganese-bearing hematite (Fe_2O_3), quartz polymorphs (SiO_2), topaz ($Al_2SiO_4(F,OH)_2$), and bixbyite (not to be confused with bixbite—the outdated name for red beryl). Bixbyite is a cubic, manganese iron oxide mineral, $(Mn, Fe)_2O_3$. It was first suggested that the coloration of red beryl was due to Mn^{2+} within the chemical structure (Nassau and Wood, 1968), though a more recent study has suggested that Mn^{3+} and possibly also Fe^{3+} incorporated into the structure give red beryl its color. In this same study, Co^{2+}, Fe^{3+}, and Ni^{3+} proposed the cause of coloration within synthetic red beryl (Shigley et al., 2001).

Chemical analyses, though limited, have been performed previously on red beryl from the Thomas Range and the Wah Wah Mountains. A hypothesis regarding the formation of the red beryl between these two localities is that the formation of red beryl is due to a beryllium-fluoride complex, which allowed the transport of beryllium in the melt, the accumulation of beryllium in-solution, and the ultimate precipitation of beryllium-rich minerals such as beryl upon the exsolution of fluorine. Once the beryllium-fluoride complex broke down (Christiensen et al., 1997). It has also been suggested that other factors may have played an indirect role in the formation of red beryl, such as faulting. Faults caused by the concurrent events of Basin and Range extension and volcanism may have allowed for surficial water to be introduced to the melt, which created preferable conditions for fluorine and beryllium to stay in solution and be transported (Wood, 1992). Other studies propose a seepage of surficial water rich in $CaCO_3$ to the melt, introducing calcium, which bonded with the fluoride in-solution to form fluorite (Christiensen et al., 1997).Once the melt became depleted in fluorine, having exsolved to topaz

and fluorite conditions for beryllium to stay in-solution became unpreferable, and precipitated to form bertrandite and/or beryl.

Objectives of Research

The aim of this study is to observe the geochemical patterns (or lack thereof) of the chromophore elements (and chromophore-like elements) of red beryl across the three localities to better understand its formation, and the conditions that allowed it to form. Analyses measuring elemental abundances will be performed on eight beryl specimens collected from the three known localities—two samples from Topaz Mountain in the Thomas Range, Utah, four samples from Paramount Canyon located within the Black Range of Gila National Forest in New Mexico, and two samples from the Ruby Violet Claims in the Wah Wah Mountains, Utah.

Hypotheses

H_0: The red beryl chromophore geochemistry of each of the three known localities are indistinguishable from each other.

H_a: The red beryl chromophore geochemistry from each of the three localities are distinguishable from one another.

Additionally, a second set of hypotheses will be assessed.

H_0: Red beryl chromophore geochemistry is indistinguishable from the chromophore chemistry of other beryl varieties

H_a: Red beryl chromophore geochemistry is distinct from the chromophore chemistry of other beryl varieties

Research Design and Methods

Laser Ablation Inductively Coupled Plasma Mass Spectrometry

To measure and compare the chemistry across the three red beryl localities. LA-ICP-MS analyses will be performed on the red beryl samples. NIST's SRM610, SRM612, and BHVO-2g will be used as standards in these analyses. The first one-inch round contains three six-sided red beryl crystals from each locality mounted in a disk of epoxy, then polished to expose the crystals. To observe any possible zonation, nine-spot, nine-spot, and ten-spot traverse from rim to core to rim were completed on the Wah Wah Mts. sample, Black Range sample, and the Topaz Mt. sample, respectively. Zonation is not an uncommon occurrence in red beryl, and several of the collected samples exhibit slight to moderate color zonation.

For the first epoxy round, each spot was ablated for ten seconds with a spot size of 85μm circle. Two sets of SRM612 and BHVO-2g analyses were performed before and after the traverse of each individual sample.

The second epoxy round contains a total of five red beryl samples—one large six-sided red beryl from Topaz Mountain, one six-sided red beryl from the Wah Wah Mountains, and three shards of red beryl from the Black Range. For this analysis, the spot size was an 85μm circle, and the analysis time was twenty-seven seconds with a total shot-count of 200. A rim-core-rim traverse of thirty-two spots was performed on the Topaz Mt. Sample, A rim-core-rim traverse of fifteen spots, as well as six spots additional spots for a total of twenty-one spots in the Wah Wah Mts. sample, and finally a total of twenty-three spots across three Black Range samples—the largest sample having eleven spots, the second largest having ten spots, and the smallest sample having two spots analyzed. Similar to the first set of analyses, the traverses and analyses of each locality was enclosed by two sets of standard analyses. In the second analysis,

BHVO-2g and NIST's SRM-610 were used as standards. Due to miscommunication, SRM-612 and SRM-610 were used for each respective analysis, though this error was corrected by recalculating one of these analyses.

A series of elements, including Li, Na, Mg, Si, K, Ca, Ti, V, Cr, Mn, Fe, Co, Ni, Cu, Ga, Rb, Sr, LREE's, and HREE's will be observed. Manganese, chromium, cobalt, and iron may play a role in the coloration of beryl (Shigley et el., 2001). Iron, manganese, titanium, and calcium may exhibit patterns across the three localities that will give insight into the geochemical chemical and physical processes of red beryl formation. Additionally, previous studies have shown red beryl being enriched in HREEs and depleted in LREEs (Alonso-Perez, Day, 2021).

Calculations

Data from both the background and samples were hand-calculated using the equation in (**Figure 2**) by the student and checked by recalculation of BHVO-2g as an "unknown" using the SRM standard, then calculating the percent error of the calculated element abundance of BHVO-2g and the official element abundance of BHVO-2g. This check was performed for both the first and second sets of analyses and double checked by separate hand-calculation and a calculation via Iolite, which concluded that the most accurate (and similar) calculations were performed by the student and Iolite.

$$True\ Standard\ Conc.\ [A]\ (ppm) * \frac{\left(\frac{[A]\ Sample\ (cps)}{[A] Measured\ Standard\ (cps)}\right)}{\left(\frac{[Si]\ Sample\ (cps)}{[Si] Measured\ Standard\ (cps)}\right)}$$

Where "[A]" is an element.

F.2: Counts per second (cps) to parts per million (ppm) equation

Background counts of each observed element were subtracted from the measured counts of the same element to give a more accurate reading. Data from the LA-ICP-MS analyses were then converted from counts per second (cps) to parts per million (ppm) and normalized to Si (**Figure 3**) using either SRM612 or SRM610 for all elements.

Results

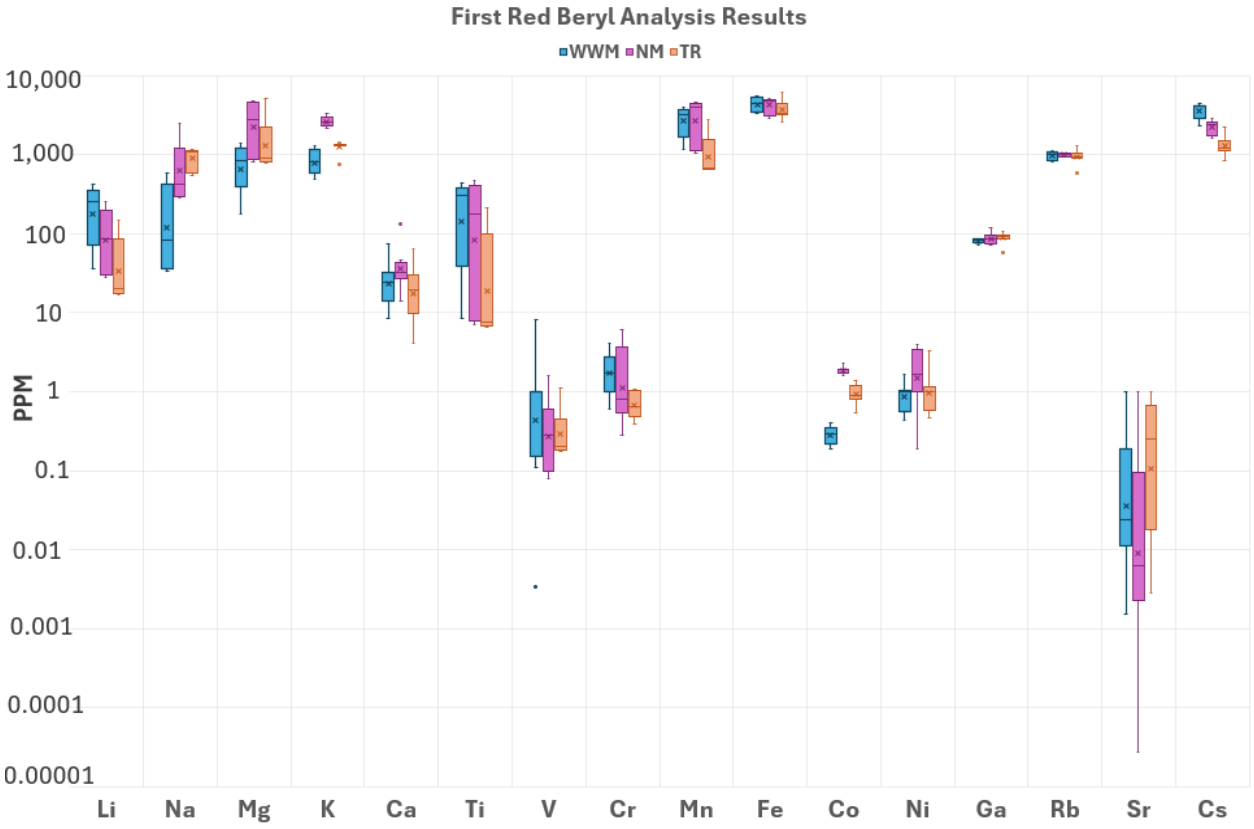

F.3: Elemental abundances in ppm of the red beryl analyses of the first epoxy round.

Almost all elements display overlap except for potassium and cobalt **(Figure 3)**. Red beryl from all localities have the highest enrichment of Mn and Fe, and depletion in Cr, V, and

Sr. Additionally, there is enrichment in Li, Na, Mg, K, Ca, Ti, Cs containing elemental abundances more than one hundred and some one thousand ppm. Zonation was observed in many of the elements analyzed, such as Fe and Mn exhibiting enrichment in the rim and depletion within the core.

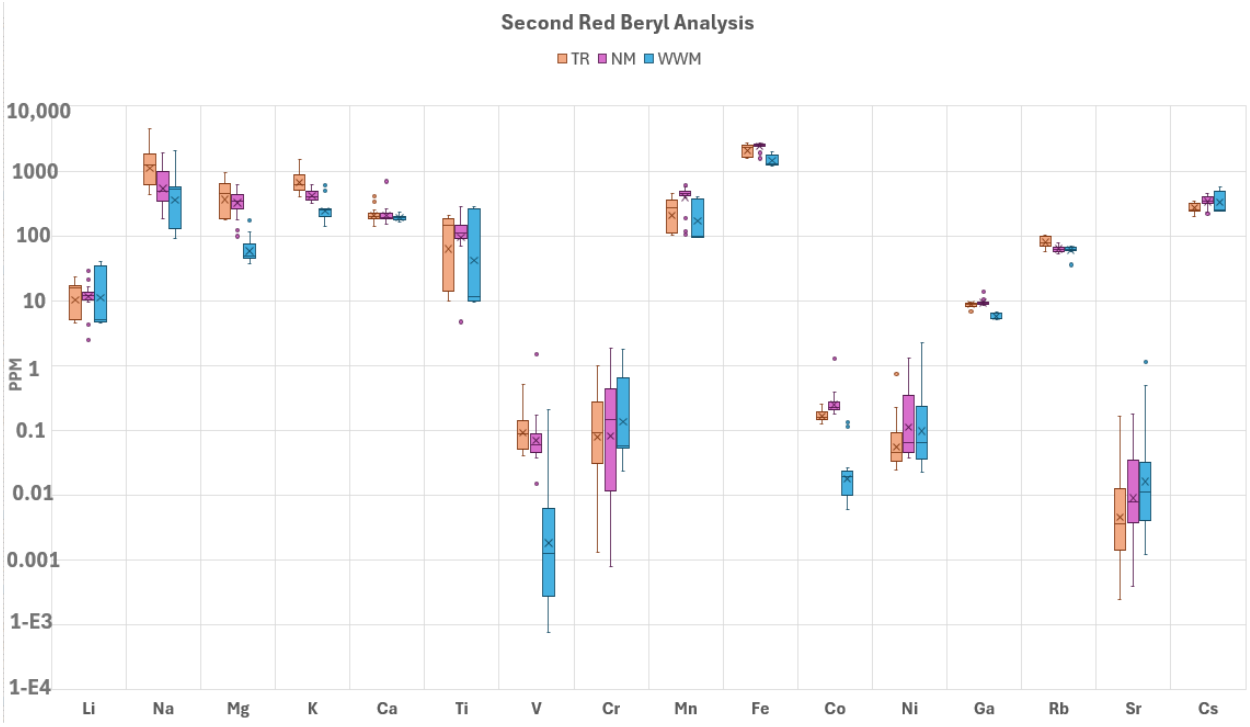

F.4: Elemental abundances in ppm of the red beryl analyses of the second epoxy round.

In the second red beryl analysis (**Figure 4**), there is enrichment in Na, K, Ca, Ti, Mn, Fe, and Cs, and depletion in V, Cr, Co, Ni, and Sr. Unlike the first red beryl analysis, there is a smaller range of elemental abundance in nearly all the elements, with the exception of V and Cr, which had many values below detection limits in both analyses. The data from both analyses were compiled into a singular dataset to compare against other varieties of beryl from Gavrilchik et al. 2023.

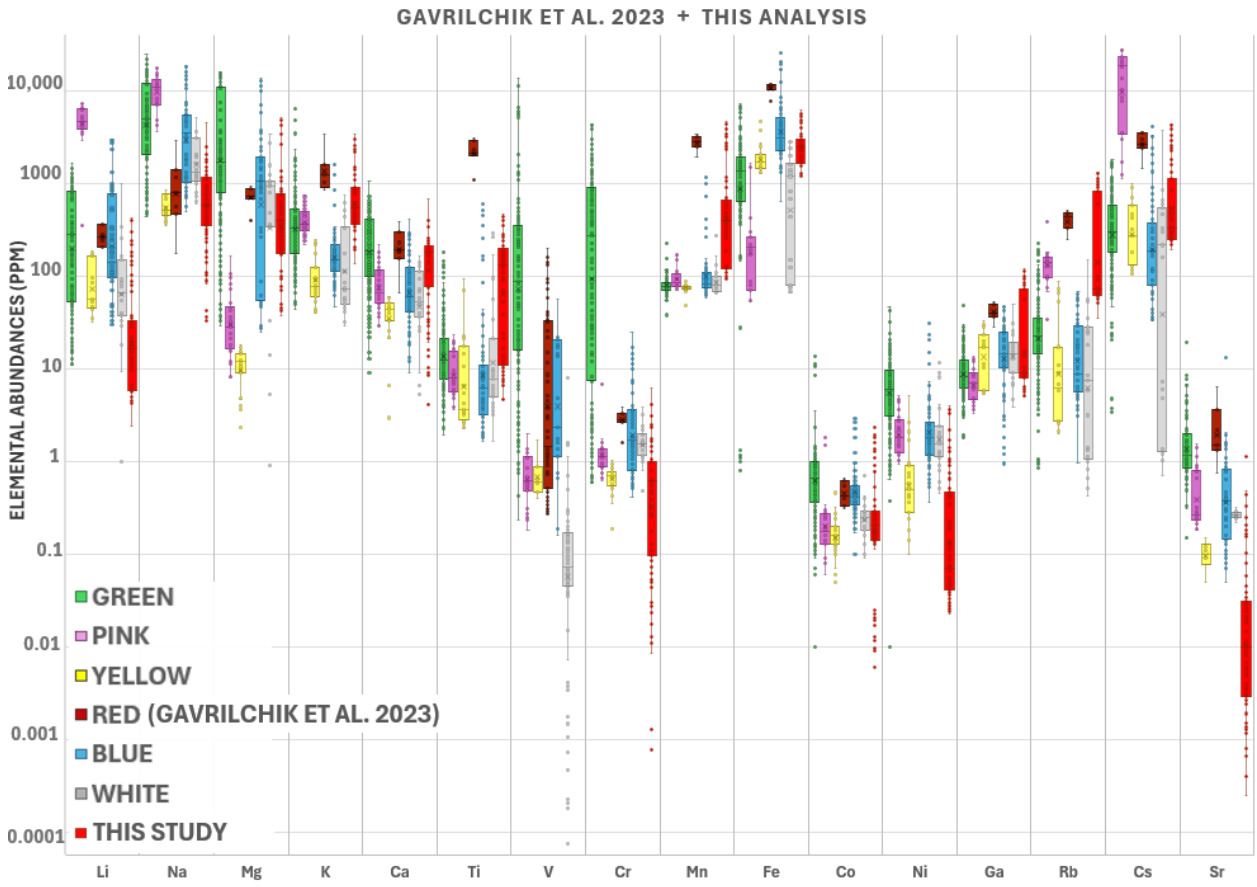

F.5: Gavrilchik et al. 2023 beryl analyses plotted with the compiled analyses of this study

For all varieties of beryl (**Figure 5**), enrichment in elements such as Na, Mg, K, Mn, Fe, and Cs can and depletion in Sr can be observed. Many beryl varieties, with the exception of green beryl, are depleted in Cr, having anywhere from around ten ppm to nearly a thousandth ppm. Green beryl, whose proposed primary chromophore is Cr, contains up to nearly ten-thousand ppm. Gavrilchik et. al. observed the highest (or second highest) enrichment of K, Ti, Mn, Fe, Ga, Rb, and Sr within their red beryl sample. Many of the red beryl abundances in both this and Gavrilchik's analysis overlap in elements with the exception of Ti, which this analysis measured nearly an order of magnitude less, V—which this analysis contained many measured abundances below detection limits, and Fe, of which both Gavrilchik et al. and this analysis had high enrichment, but this analysis recorded a lower and larger range of abundances for Fe, (as

well as Mn). Both red beryl analyses recorded enrichment in Cs, but not nearly as much as pink beryl, surpassing the other beryl varieties by several orders of magnitude. Pezzottaite, a type of Cs-rich pink beryl, is said to receive its coloration from Cs within the crystal structure.

DISCUSSION

The high enrichment of Mn and Fe observed within both this set of red beryl analyses and the Gavrilchik et al. analyses is consistent with proposed coloring agents for red beryl. There is also enrichment in Rb and Cs reflecting previous observations of Rb and Cs enrichment in topaz rhyolites (SOURCE). A traverse of one sample was recorded in the Gavrilchik et al. analyses, which may account for the small range it exhibits in comparison to the larger range the red beryl of this analysis exhibits. Samples from the Wah Wah Mountains and the Black Range, especially those of the first epoxy round, show evidence of significant visual zonation, which is reflected chemically in the rim-core-rim traverses. The Topaz Mountain sample of the first epoxy round shows weak zoning, but the Topaz Mountain sample of the second epoxy round shows much stronger zonation (**Appendix A, B, C**). It is to be noted that the proposed coloring agents of red beryl are more enriched in the rim and depleted within the core of the two pictured samples (**Figure 6**).

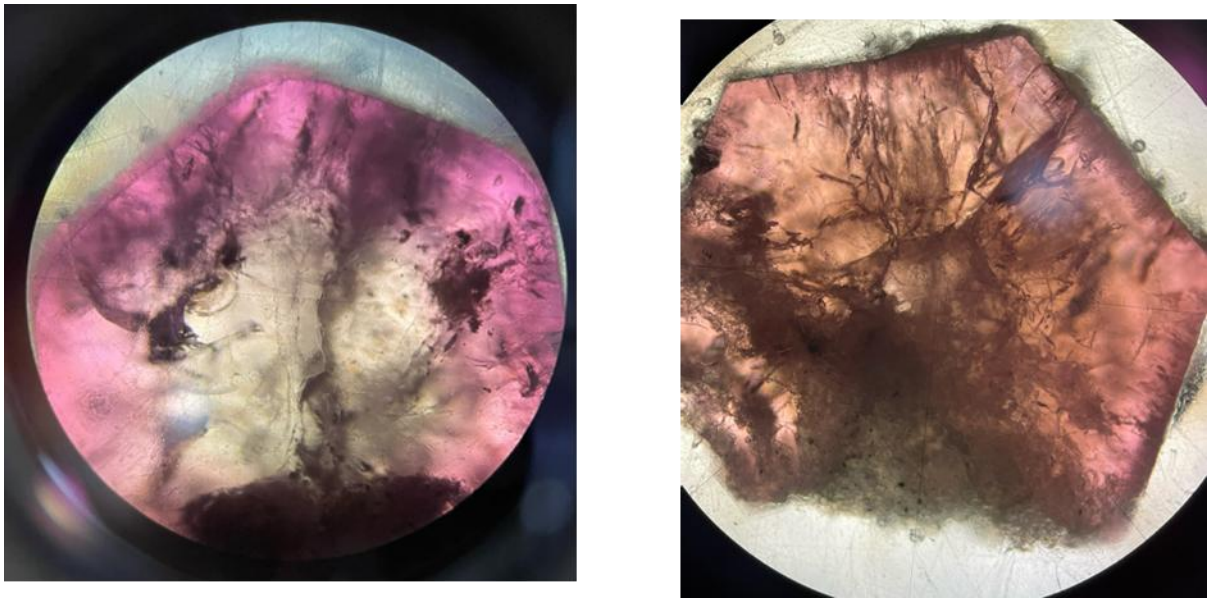

F.6: Wah Wah Mts. and Black Range samples of analysis one under petrographic microscope.

Given the range of color red beryl can have (recall it can be pink, red, magenta, purple) the question is raised of establishing what, if any, difference distinguishes pink beryl from red beryl. Pink beryl can receive coloration from either Cs or Mn. Cs-rich pink beryl is called Pezzottaite and Mn-rich pink beryl is called Morganite. Red beryl, though historically high in Cs, does not get its coloration from Cs, however, both red beryl and morganite both received coloration through Mn. There has been conflicting ideas in previous literature, suggesting the separation is marked by the charge of Mn (Mn^{2+} or Mn^{3+}), though this has not been clear. There doesn't seem to be one definite answer for which charge of Mn is responsible for which beryl, or if there is even any difference at all. This is something that remains to be answered. Red beryl is the only type of beryl known to form in topaz rhyolites and has not been recorded

in any other environment. Morganite primarily forms in pegmatites and has a different trace elemental profile than red beryl.

Conclusions

In the first study of its kind, several samples from all three localities have been observed to better understand red beryl and its chemical characteristics. Of the eight analyzed samples of this study, and the sample analyzed of the Gavrilchik et. al 2023 study, it can be observed that all red beryl has a nearly indistinguishable chromophore profile, with a range of abundances between each element observed due to zonation. Though generally all beryl is enriched and depleted in many of the observed elements, red beryl contains many elemental abundances orders of magnitude higher than the other beryl varieties and some elemental abundances orders of magnitude lower than the other beryl varieties. It can be concluded that though sharing some similarities with other beryl varieties, red beryl is not indistinguishable from other beryl varieties, Studying the major, minor, and trace elements of the red beryl, as well as how they vary across both the individual crystals and each of the three known localities, can give us insight into how it formed, as well as information for discovering new localities.

Acknowledgements

Carnegie Institute of Science: Timothy Mogk, Lori Willhite and Michelle Jordan.

Dr. Philip Piccoli

Dr. Richard Ash

Dr. S.G. Skublov, Konstantina Gavrilchik

Thank you so much for your help and guidance!

Bibliography

Abbott, J. T.; Best, M. G.; Morris, M. T.; Geologic Map of the Pine Grove-Blawn Mountain Area, Beaver County, Utah, **1983** **10.3133/i1479**

Alonso-Perez, R.; Day, J. M. D.; Rare Earth Element and Incompatible Trace Element Abundances in Emeralds Reveal Their Formation Environments. *Minerals*, *11*, 513 **2021**

Baker, J. M.; Genesis of Red Beryl in Topaz Rhyolites in Starvation Canyon, Thomas Range, Utah. Dissertation for Master of Science (Geology), Brigham Young University, **1998**

Blakemore, D. R.; Applications of Laser Ablation Inductively Coupled Plasma Mass Spectrometry to Problems in Mineral Resource Geology. Dissertation for Doctor of Philosophy (Earth and Environmental Sciences), University of Michigan, **2024**

Christiansen, E. H.; Bikun, J. V.; Sheridan, M. F.; Burt, D. M.; Geochemical Evolution of Topaz Rhyolites from the Thomas Range and Spor Mountains, Utah. *American Mineralogist*, *69*, 223–236, **1984**

Christiansen, E. H.; Keith, J. D.; Thompson, T. J.; Origin of Gem Red Beryl in Utah's Wah Wah Mountains. *Mining Engineering*, 37–41, **1997**

Edge, C.; *What Gemstone is Found in Utah that is Rarer than Diamond and More Valuable than Gold?* Utah Geological Survey, **2002**

Gavrilchik, A. K.; Skublov, S. G.; Kotova, E. L.; Trace Element Composition of Beryl from the Sherlovaya Gora Deposit, Southeastern Transbaikal Region, Russia. *Geology of Ore Deposits*, Vol. 64, p. 442-451, **2023**

Hanser, C. S.; Hager, T; Botcharnikov, R.; Incorporation and Substitution of Ions and H2O in the Structure of Beryl. *European Journal of Mineralogy*, *36*, 449–473, **2024**

Hanser, C. S.; Vullum, P. E.; Johannes van Helvoort, A. T.; Schmitz, F. D; Hager, T; Botcharnikov, R.; Holst, B.; Atomic Resolution Transmission Electron Microscopy Visualisation of Channel Occupancy in Beryl in Different Crystallographic Directions. *Springer* **2024**.

Hintze, L. F.; Fitzhugh, D. D. Geology Map of the Wah Wah Mountains North 30' x 60' Quadrangle and Part of the Garrison 30' x 60' Quadrangle, Southwest Millard County and Part of Beaver County, Utah, **2002**.

Jaskula, B. W.; Beryllium. *Mineral Commodity Summaries*, **2024**

Karampelas, S.; Al-Shaybani, B.; Mohamed, F.; Sangsawong, S.; Al-Alawi, A.; Emeralds from the Most Important Occurrences: Chemical and Spectroscopic Data. *Minerals*, *9*, 561, **2019**

Keith, J. D.; Christiansen, E. H.; Tingey, D. G.; Geological and Chemical Conditions of Formation of Red Beryl, Wah Wah Mountains, Utah. *Utah Geological Association*, *23*, 155–169, **1994**

Lindsey, D. A.; Geologic Map and Cross-Sections of Tertiary Rocks in the Thomas Range and Northern Drum Mountains, Juab County, Utah, **1979**

Lum, J. E.; Viljoen, F.; Carincross, B.; Frei, D.; Mineralogical and Geochemical Characteristics of Beryl (Aquamarine) from the Erongo Volcanic Complex, Namibia. *Journal of African Earth Sciences*, Vol. 124, p. 104-125, **2016**

Michayluk, M. C.; New Red Beryl Find in Paramount Canyon; Socorro, NM, **2016**; p 519.

Nassau, K., and Wood, D.L.; An Examination of Red Beryl from Utah. *American Mineralogist*, v. *53*, p. 801-806, **1968**

Peretti, A.; Armbruster, T.; Gunther, D.; Grobety, B.; Hawthorne, F. C.; Cooper, M. A.; Simmons, W. B.; Falster, A. U.; Rossman, G. R.; Laurs, B. M.; The Challenge of the

Identification of a New Mineral Species: Example "Pezzottaite". *Contributions to Gemology*, Vol. *3*, **2004**

Shigley, J. E.; McClure, S. F.; Cole, J. E.; Koivula, J. I.; Lu, T.; Shane, E.; Demianets, L. N.; Hydrothermal Synthetic Red Beryl from the Institute of Crystallography, Moscow. *Gems & Gemology* , 42–55, **2001**

Shigley, J. E.; Foord, E. E.; Gem Quality Red Beryl from the Wah Wah Mountains, Utah. *Gems and Gemology*, 208-221, **1984**

Staatz, M. H.; Geology of the Beryllium Deposits in the Thomas Range Juab County, Utah. *Contributions to Economic Geology, Geological Survey Bulletin 1142–M,* **1963**

Staatz, M. H.; Carr, W. J. Geology and Mineral Deposits of the Thomas and Dugway Ranges Juab and Tooele Counties, Utah. *Geological Survey Professional Paper, 415,* 1–189. **1964**

Webster, J. D. Partitioning of F between H2O and CO2 Fluids and Topaz Rhyolite Melt. *Contributions to Mineralogy and Petrology, 104,* 424–438, **1989**

Wolfang, E. E.; When Batholiths Exploded: The Mogollon-Datil Volcanic Field, Southwestern New Mexico, **2008**

Wood. S.A.; Theoretical Prediction of Speciation and Solubility of Beryllium in Hydrothermal Solution to 300° C at Saturated Vapor Pressure: Application to Bertrandite/Phenakite Deposits. *Ore Geology Reviews*, Vol. 7*,* p. 249-278, **1992**

Appendix A: Elemental Data of Red Beryl from the Black Range, New Mexico

CONC. (PPM)		Li	Na	Mg	K	Ca	Ti	V	Cr	Mn	Fe	Co	Ni	Cu	Ga	Rb	Sr	Cs
E.	NM1 [RIM]	220	2519	4855	2374	135	449	1.6	4.1	4387	4789	1.9	4.0	14	102	1064	0.21	2749
	NM2	102	285	3451	2280	40	218	0.24	0.28	3920	5074	1.9	3.4	11	86	961	0.01	2316
	NM3	80	417	2689	2632	47	162	0.30	0.46	4064	5041	2.0	0.19	11	83	1032	0.00	2370
R	NM4	28	1119	879	3044	40	7.8	0.10	6.1	1081	3163	1.8		16	73	924	0.02	1595
N	NM5 [CORE]	28	1127	800	2972	30	7.2	0.10	0.64	1054	2893	1.6	0.00	18	73	937		1666
D	NM6	31	1261	877	3388	14	8.0	0.08	0.63	1167	3050	1.9		18	76	1057	0.00	1798
	NM7	88	351	2822	2554	32	179	0.28	0.84	4672	5241	2.3	1.7	10	87	1046	0.00	2421
1	NM8	180	301	4585	2331	25	364	0.50	0.79	3949	4891	1.6	3.4	12	85	993	0.05	2412
	NM9 [RIM]	251	295	4518	2173	32	467	0.74	3.34	4503	4873	1.9	2.4	17	119	1019.4	0.00	2932
	NM1 lg start	11	451	390	482	236	101	0.07		601	2605	0.27	0.35	1.1	9.3	77	0.00	443
	NM2	10	478	320	434	180	92	0.07	0.01	479	2466	0.23	0.11	1.0	10	69	0.16	417
E	NM3	11	586	341	424	194	89	0.14		494	2554	0.23	0.05	0.98	9.1	67	0.01	400
P	NM4	11	841	434	488	690	96	0.16	0.01	569	2604	1.3	0.08	1.1	9.1	75	0.00	430
O	NM5	10	1229	398	540	241	92	0.08	0.03	541	2618	0.25	0.13	1.0	9.1	70	0.00	404
X	NM6	11	400	264	364	185	91	1.5		441	2425	0.22	0.20	0.98	8.7	59	0.01	343
Y	NM7	12	353	264	349	153	109	0.04		491	2578	0.38	0.06	1.1	8.9	59	0.01	326
	NM8	11	358	209	315	187	101	0.09	0.00	391	2411	0.20	0.07	1.1	8.7	52	0.00	300
R	NM9	9.5	1914	177	585	218	69	0.04	0.29	188	1903	0.24	0.47	1.9	8.8	54	0.03	231
O	NM10 lg end	16	965	337	449	175	155	0.09	1.3	420	2534	0.20	1.32	0.89	8.9	54	0.18	298
U	NM11 med start	21	1793	470	565	224	222	0.06	0.18	440	2652	0.29	0.48	1.0	9.8	60	0.04	322
N	NM12	28	184	611	322	187	286	0.06		435	2632	0.21	0.07	2.6	14	64		400
D	NM13	22	232	597	369	189	250	0.06		461	2663	0.28	0.04	1.6	10	65		352
	NM14	13	375	469	395	189	147	0.05		458	2605	0.20	0.04	1.3	9.5	66		351
2	NM15	13	254	417	395	220	130	0.05		470	2537	0.23	0.04	1.2	9.0	64	0.01	350
	NM16	17	254	506	362	166	183	0.04		449	2610	0.21	0.05	1.3	9.4	61	0.02	332
	NM17	13	603	333	341	167	125	0.04		399	2454	0.19	0.04	1.1	8.9	56	0.01	317
	NM18	14	574	357	391	216	135	0.04		429	2535	0.21	0.05	1.2	9.3	58	0.01	319
	NM19	13	322	317	348	201	131	0.05	0.31	420	2545	0.21	0.41	1.3	9.3	57	0.00	320
	NM20	12	340	313	376	172	113	0.17		469	2543	0.28	0.05	1.2	9.0	61		342
	NM21 med end	10	479	287	381	184	93	0.05		448	2478	0.21	0.04	1.1	8.7	62	0.01	362
	NM22 sml start	4.3	1367	121	606	259	4.7	0.01	0.12	119	1572	0.22	0.05	2.2	8.3	78	0.06	303
	NM23 sml end	2.4	977	99	429	213	4.7	0.07	1.8	104	1661	0.17	1.28	1.1	8.4	56	0.02	222

*Blank spaces denote values below detection limits.

Appendix B: Elemental Data of Red Beryl from the Thomas Range, UT

	CONC. (PPM)		Li	Na	Mg	K	Ca	Ti	V	Cr	Mn	Fe	Co	Ni	Cu	Ga	Rb	Sr	Cs
	TR1	[RIM]	147	630	5079	1410	30	214	1.1	0.39	2628	5729	1.4	0.67	11	107	1294	0.01	2243
E.	TR2		19	1107	908	1319	10	6.6	0.18		670	3381	0.97	0.46	6.9	94	934	0.03	1203
	TR3		17	1095	773	1309	4.1	6.5	0.18	1.1	678	3261	1.1		6.1	88	916	0.06	1148
R	TR4		20	1096	793	1271	16	7.4	0.20	0.47	662	3412	0.81		8.3	89	902	0.00	1146
N	TR5	[CORE]	67	547	1173	768	29	53	0.18	0.80	920	2596	0.53	0.51	5.3	57	597	0.33	856
D	TR6		23	1083	852	1332	9	7.2	0.18	0.51	707	3464	0.91		9.0	87	916	0.00	1136
	TR7		108	558	4318	1308	64	184	0.70	1.1	2735	6181	1.4	3.3	9.4	101	1109	0.44	1792
1	TR8		18	1171	892	1320	19	7.6	0.30	0.54	688	3372	0.92	1.4	6.2	94	975	0.25	1308
	TR9		17	1157	845	1309	21	7.5	0.28	0.65	662	3234	0.78		6.4	94	998	0.00	1308
	TR10	[RIM]	164	939	4849	1432	80	225	1.5	0.63	2528	5446	1.3	3.7	14	115	1335	0.15	2580
	TR1	[RIM]	21	568	947	530	200	200	0.14	0.07	296	2396	0.17	0.05	1.2	9.5	78	0.01	349
	TR2		20	1161	770	507	167	189	0.13	0.99	283	2378	0.17	0.14	0.94	9.4	72	0.02	325
	TR3		17	479	590	444	336	154	0.12	0.02	256	2301	0.15	0.10	1.1	8.9	62	0.00	285
	TR4		16	529	428	445	179	145	0.51	0.09	294	2478	0.16	0.03	1.1	9.0	61		295
	TR5		17	915	481	508	140	166	0.13	0.06	379	2568	0.22	0.03	1.0	9.1	68		334
	TR6		17	607	541	534	184	181	0.23	0.04	420	2608	0.22	0.03	0.90	9.2	72	0.00	331
	TR7		18	668	568	544	188	182	0.24	0.17	411	2661	0.21	0.02	0.94	9.2	73	0.01	321
E	TR8		18	716	642	585	180	197	0.14		447	2725	0.23	0.03	0.87	9.3	75	0.00	309
P	TR9		16	4519	470	1522	351	142	0.11	0.40	306	1812	0.15	0.74	0.66	6.7	60	0.17	195
O	TR10		18	864	653	631	185	195	0.17	0.13	406	2654	0.21	0.10	0.79	9.1	76	0.00	289
X	TR11		5.6	1890	194	937	402	17	0.06	0.00	118	1754	0.15	0.09	1.5	8.4	102	0.00	244
Y	TR12		4.7	1844	180	919	218	10	0.05	0.03	100	1621	0.15	0.05	1.2	8.6	100	0.00	244
	TR13		4.6	1913	186	902	230	38	0.05	0.10	100	1631	0.15	0.04	1.1	8.3	100	0.01	243
R	TR14		4.8	1831	182	893	204	10	0.04		101	1641	0.15	0.03	1.2	8.3	99	0.01	246
O	TR15		5.0	1778	188	875	253	12	0.05	0.11	104	1570	0.13	0.06	1.3	8.1	96	0.04	236
U	TR16	[CORE]	4.9	1851	179	870	254	9.9	0.04	0.31	102	1599	0.13	0.05	1.2	8.1	97	0.00	248
N	TR17		4.5	1755	180	868	226	189	0.05		122	1998	0.13	0.11	1.1	8.2	95	0.00	236
D	TR18		4.8	1790	185	884	210	10.3	0.04		100	1578	0.15	0.03	1.2	8.1	97	0.00	239
	TR19		5.0	2079	184	876	219	21.4	0.05		101	1565	0.14	0.23	1.2	8.0	95	0.00	245
2	TR20		5.8	1777	198	873	242	13.8	0.05		112	1641	0.14	0.04	1.6	8.5	96	0.01	241
	TR21		6.6	1761	173	834	196	14.3	0.05		111	1687	0.13	0.05	1.9	8.2	91		223
	TR22		6.1	1700	242	833	210	24.0	0.06		129	1642	0.14	0.05	1.3	8.2	92	0.01	251
	TR23		5.1	1864	218	923	220	11.0	0.05		111	1626	0.16	0.09	1.4	8.2	102	0.00	257
	TR24		4.7	1913	226	910	224	11.5	0.06		119	1592	0.16	0.03	1.3	8.3	101		258
	TR25		17	806	744	613	198	188	0.15		414	2622	0.21	0.10	0.81	9.1	78	0.00	312
	TR26		17	717	719	588	196	180	0.14		386	2562	0.20	0.05	0.86	9.4	75	0.01	323
	TR27		17	1284	650	547	183	167	0.16	0.01	369	2605	0.18	0.04	0.97	9.1	73	0.00	351
	TR28		16	630	481	469	148	150	0.14		321	2396	0.17	0.03	0.93	8.9	64	0.00	306
	TR29		16	567	436	434	168	146	0.12		307	2402	0.16	0.06	1.1	8.8	62	0.00	290
	TR30		15	443	463	398	168	140	0.07		259	2378	0.15	0.03	1.1	8.8	57	0.02	273
	TR31		17	425	572	421	192	159	0.07		291	2459	0.15	0.04	1.2	9.3	63	0.01	280
	TR32	[RIM]	23	548	642	462	179	207	0.16		287	2384	0.25	0.04	1.2	9.6	69	0.03	325

*Blank spaces denote values below detection limits.

Appendix C: Elemental Data of Red Beryl from the Wah Wah Mountains, UT

CONC. (PPM)	Li	Na	Mg	K	Ca	Ti	V	Cr	Mn	Fe	Co	Ni	Cu	Ga	Rb	Sr	Cs
WWM 1 [RIM]	419	83	179	585	29	403		4.1	3938	3426	0.41		3.5	81	815	0.02	4446
WWM 2	314	37	830	622	14	369	0.11	1.8	3320	5078	0.39	0.92	2.6	86	863	0.10	4080
WWM 3	242	33	1365	837	14	293	0.21	0.6	3414	5584	0.19	1.1	3.5	86	1094	0.00	4113
WWM 4	39	586	502	1313	34	10		2.3	1245	3387	0.27		10	74	1075	0.01	2510
WWM 5 [CORE]	36	560	487	1254	30	9		2.5	1187	3458	0.24	0.44	9.8	72	1036	0.02	2318
WWM 6	133	330	1054	1106	24	149		0.80	2340	4523	0.33	1.7	7.8	80	1120		3351
WWM 7	252	35	1411	800	24	300	0.00	1.3	3266	5486	0.29	1.0	4.4	85	1026	0.03	4081
WWM 8	303	43	844	590	8	354		1.5	3162	4972	0.20	0.65	2.8	83	842	0.01	3920
WWM 9 [RIM]	399	268	308	484	76	438	8.07	3.1	3922	3941	0.30	0.48	4.3	82	851	0.34	4290
WWM1 [RIM]	40	104	46	203	178	286			393	1587	0.02	2.2	0.32	6.4	68		546
WWM2	35	103	78	192	196	262	0.00	0.10	345	1786	0.02	0.07	0.30	5.9	66	0.08	483
WWM3	4.4	1485	46	494	232	10	0.00	1.6	95	1299	0.01	0.99	0.76	5.3	62	0.02	244
WWM4	33	160	92	197	197	246	0.00	0.06	354	1890	0.02	0.43	0.34	6.0	63	0.00	448
WWM5	5.0	2058	48	599	201	13	0.00	0.26	100	1275	0.11	0.44	0.79	5.2	62	0.02	245
WWM6	4.6	595	44	259	215	9.6	0.00	0.02	94	1252	0.02	0.07	0.77	5.6	59	1.13	242
WWM7	4.7	551	48	255	210	9.8	0.00	1.7	96	1261	0.02	1.4	0.90	5.2	59	0.00	247
WWM8 [CORE]	4.8	523	50	252	178	11	0.04		97	1262	0.01	0.04	0.77	5.1	59	0.01	246
WWM9	4.6	548	45	254	181	9.5	0.21		95	1202	0.01	0.08	0.75	5.1	57	0.00	244
WWM10	4.6	531	46	254	211	9.7	0.05		93	1210	0.01	0.02	0.74	5.3	58		248
WWM11	4.7	773	47	258	193	9.8	0.00	0.05	95	1239	0.01	0.06	0.75	5.4	61		251
WWM12	30	111	171	205	171	218			336	1971	0.02	0.04	0.34	6.4	70	0.01	480
WWM13	33	116	101	191	165	239	0.00		363	1817	0.13	0.03	0.33	6.4	66	0.02	481
WWM14	38	139	70	204	201	275			403	1624	0.03	0.03	0.33	6.5	70	0.01	568
WWM15 [RIM]	5.0	536	50	256	186	11	0.00	0.05	99	1250	0.01	0.09	0.74	5.3	59	0.49	251
WWM16	4.9	537	37	251	170	10			97	1197	0.01	0.04	0.76	5.2	59		251
WWM 17	35	309	43	138	173	275	0.01		396	1743	0.02	0.02	0.60	6.4	36		425
WWM18	33	281	115	198	179	251	0.00		369	1901	0.03	0.04	0.92	6.6	69	0.03	471
WWM19	38	89	70	194	193	277			387	1726	0.02	0.05	0.33	6.4	68	0.00	487
WWM20	4.8	859	43	255	180	11	0.00		98	1214	0.01	0.07	0.73	5.3	58	0.00	248
WWM21	4.9	545	46	250	195	11	0.00	0.05	96	1248	0.01	0.12	0.77	5.0	58		244

*Blank spaces denote values below detection limits.

Appendix D: Locality Overview

Topaz Mountain, Thomas Range, Utah

Overview

The Thomas Range in west-central Utah is approximately fifty miles northwest of the town of Delta. It is characterized by three different felsic eruptions that occurred in the upper Miocene. The Thomas Range is immediately surrounded by the Pleistocene deposits of Lake Bonneville and is adjacent to Fumarole Butte—a cinder cone remnant from the Pleistocene and one of many tertiary basaltic/andesitic volcanoes in Utah caused by the events of Basin and Range extension. Due to these events, as well as the events of the Sevier Orogeny, Cambrian sedimentary rocks have been uplifted around the area and marking the initial horsts and grabens of the basin and range province that dominates Nevada.

The three eruptions make up the Topaz Mountain Rhyolite and include interbedded tuff between each eruption. According to a K-Ar dating study, it was discovered that the ages of the various rhyolite flows occurred anywhere from approximately six to eight million years ago (Lindsey, 1979). The Topaz Mountain Rhyolite includes porphyritic alkaline rhyolite flows and domes, with mineral assemblages of quartz (christobalite, tridymite) , biotite, sanidine, plagioclase, topaz, garnet, red beryl, bixbyite, and pseudobrookite, opal, amethyst, fluorite, Mn-hematite, uranophane, amongst other accessory minerals, which occur in either the vertical fractures caused by the cooling and contraction of the rhyolite, or in lithophysal vugs (void spaces within the rhyolite formed by gas bubbles in the melt, having thin concentric shells within the vug), within the rhyolite (Lindsey, 1979). Many of these minerals, including red beryl, topaz, sanidine, quartz, garnet, Mn-hematite, and bixbyite occur in both the lithophysae and the vertical shrinkage fractures at this locality.

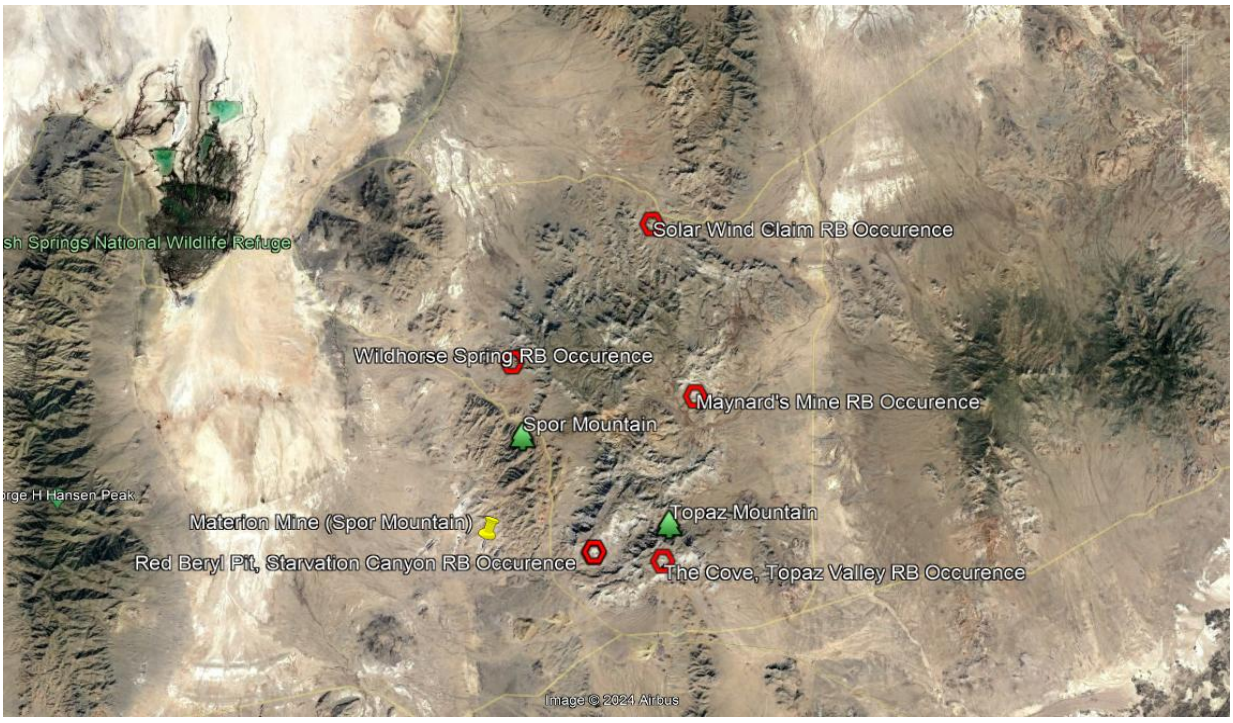

F.2: Google satellite imagery of the red beryl localities in the Thomas Range. Also shown is the location of Spor Mountain and the Materion Mine.

Spor Mountain (**F.2**) is a world-renowned producer of beryllium that is currently under management by the Materion Corporation. Spor Mountain is arguably the world's largest known beryllium deposits and producers. It is also worth noting that the rhyolite at Spor Mountain is not classified as the Topaz Mountain Rhyolite of the upper Miocene, nor does it export beryl as its main ore source. Materion Mine extracts bertrandite ($Be_4Si_2O_7(OH)_2$), a beryllium mineral that often forms as a result of hydrothermal alteration of beryl. Lower Miocene rhyolite flow of Spor Mountain likely formed through the beryllium-fluorine complex, as it contains a similar mineral assemblage as the beryl-bearing topaz rhyolites of Topaz Mountain, most notably fluorite, which was observed to co-occur in nearly all samples that contained bertrandite (Staatz, 1963). The Spor Mountain formation includes a porphyritic rhyolite member, characterized by the same traits listed above. Underlying the porphyritic

rhyolite member is the beryllium tuff member—a stratified, tan, vitric tuff and tuffaceous breccia. The beryllium tuff member also contains epiclastic tuffaceous sandstone, many clasts of carbonate rocks, and some clasts of quartzite and other volcanics. It also includes several altered minerals, including fluorite and K-Spar that have been hydrothermally altered to clay (Lindsey, 1979).

Occurrences of red beryl have been documented in both scientific research and by amateur rockhounds to not only occur at Topaz Mountain, but at several other locations around the Thomas Range, including Starvation Canyon, Wildhorse Spring, the Solar Wind claim and Maynard's Mine (Baker, 1998).

Wah Wah Mountains, Utah (Ruby Violet Mine)

Overview

The Wah Wah Mountains are a range in southwest Utah, world renowned for producing high-quality, gem-grade red beryl. It is the only of the three red beryl localities that has produced gem-grade red beryl (Shigley et al., 1984). The minerals of this locality are hosted in the early Miocene Blawn Formation rhyolite (Abbott et al., 1983). The samples from this locality used in this study were purchased at a local gem and mineral store in Cedar City, Utah.

The samples analyzed from this locality were mined by the Harris family, who originally owned and operated the Ruby Violet Mine from the 1970's to the 1990's. The specimens found at the Wah Wah Mountains locality differ from both the Thomas Range and Black Range localities in not only quality, but color and crystal habit. Red beryl from the Wah Wah Mountains is sometimes elongated on the c-axis. The color ranges anywhere from hot pink to blood red to even purple. These crystals have also been documented to sometimes exhibit a trapiche pattern—a rare growth pattern in beryl described as a six-pointed starburst

(not to be confused with asterism and chatoyancy). Red beryl from this locality is often visually and chemically zoned, having tan/faded cores and bright red/pink rims. This is not uncommon for red beryl, as zonation has been observed commonly at other localities also.

Red beryl of the Wah Wah Mountains form solely within or along sub-vertical shrinkage fractures, and do not form in lithophysal cavities (Keith et al., 1994). It has been observed that the rhyolite host rock at this locality is enriched in Rb, Nb, Y, and Be, with levels around twenty parts per million, and depleted in Ti, Sr, and Ba (Keith et al., 1994). The red beryl crystals are either found embedded in kaolin, or adjacent to the shrinkage fractures, embedded in the rhyolite. Co-occurring minerals include topaz, bixbyite, tridymite, sanidine, and cristobalite (Christiansen et al., 1997).

In terms of tectonic history, the Wah Wah Mountains have a similar origin to the Thomas Range—having formed from the ongoing events of slab-rollback volcanism during the early Miocene.

Paramount Canyon of the Black Range, New Mexico

Overview

The Paramount Canyon locality is characterized by the Taylor Creek Rhyolite, with minerals including red beryl, bixbyite, hematite, quartz, sanidine, and pseudobrookite. The Taylor Creek Rhyolite hosts siliceous volcanics from the middle Tertiary and is part of the Mogollon-Datil Volcanic Field (Elston, 2008). This volcanic field, similar to the other red beryl localities, formed during the events of slab-rollback during the Eocene-Miocene. The red beryl in this locality occurs solely within lithophysae. Unlike the two Utah localities, the color of the beryl is much lighter; a light pink/salmon color but added here as it has been described previously. Visible and chemical zonation also occurs with the red beryl from this locality.

Appendix E: Locality Observations

Topaz Mountain (Thomas Range)

It is worth noting that the samples collected from the Thomas Range are solely from the Cove area of Topaz Mountain within the area of the BLM land, not the pay-to-dig site. Within the washes of the Cove, clear, terminated topaz can be found ranging anywhere from a few millimeters to a few centimeters in length. Within vuggy cobbles and boulders, high-quality honey-colored topaz can be found. Towards the base of the Cove, it is not uncommon to see flow-banding in rhyolite. The rhyolite also contains amygdaloidal layers, which alternate with less amygdaloidal rhyolite and stratified tuff up the mountain.

Both samples were found within adits in the mountain surrounding the Cove. The sample from the smaller adit, which will from here on be referred to as RB_TM-1, was found in a vertical fracture (at around three or four feet in height) filled with kaolinite. Within the clay-filled vertical fractures were small areas about--an inch or two in diameter--of brownish clay. The clay--possibly iron-stained kaolinite or perhaps another type of clay mineral such as smectite. These areas of brown clay contained large, double-terminated clusters of topaz, which were not as gemmy as the topaz within the lithophysae. This type of topaz, which will be referred to as sandy topaz, contains substantial amounts of rhyolite and clay in and around the crystal itself.

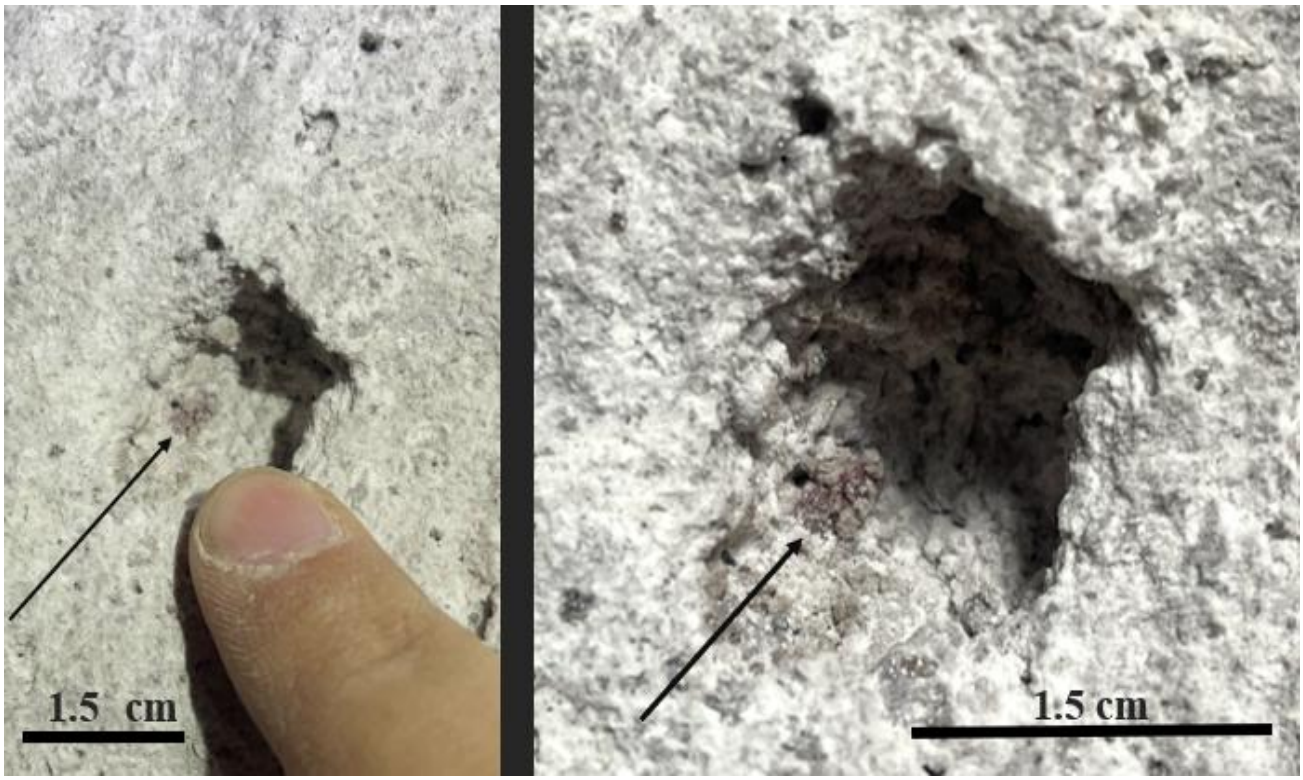

Figure 7: A lithophysal cavity from Topaz Mountain with a red beryl in-situ.

RB_TM-2 came from a larger adit from higher up the mountain. This sample was extracted from one of the lithophysae within the adit (**Figure 6**). The lithophysae were abundant in gemmy, euhedral minerals such as quartz, sanidine, honey-colored topaz, clear topaz, and bixbyite. Like RB_TM-1, RB_TM-2 was more of a mulberry color in the areas of the crystal less obscured by rhyolite and clay inclusions. Also, like RB_TM-1, the lithophysal sample is a stubby hexagonal prism, shortened along the long axis, and contains a large amount of mineral and rock inclusions within the crystal itself, including rhyolite and bixbyite. RB_TM-2 is only five millimeters in length, and two and a half millimeters in height.

Paramount Canyon (Black Range, NM)

On a cliffside of Paramount Canyon, a hematite vein running roughly north-south has been observed, and there is an outcrop of red beryl about two hundred feet west of this vein (Michayluk, 2016). The vein displayed an abundance of euhedral, plated hematite, as well as euhedral bixbyite (**Figure 7**). Bixbyite has a cubic habit, with beveled corners that come to a three-sided point as well as beveled edges.

Figure 8: Hematite (left) and bixbyite (above) within lithophysae from Paramount Canyon.